Joint Resources and Workflow Scheduling in UAV-Enabled Wirelessly-Powered MEC for IoT Systems

Yao Du, Kun Yang, *Senior Member, IEEE*, Kezhi Wang, Guopeng Zhang, Yizhe Zhao, and Dongwei Chen

***Abstract*—This paper considers a UAV-enabled mobile edge computing (MEC) system, where a UAV first powers the Internet of things device (IoTD) by utilizing Wireless Power Transfer (WPT) technology. Then each IoTD sends the collected data to the UAV for processing by using the energy harvested from the UAV. In order to improve the energy efficiency of the UAV, we propose a new time division multiple access (TDMA) based workflow model, which allows parallel transmissions and executions in the UAV-assisted system. We aim to minimize the total energy consumption of the UAV by jointly optimizing the IoTDs association, computing resources allocation, UAV hovering time, wireless powering duration and the services sequence of the IoTDs. The formulated problem is a mixed-integer non-convex problem, which is very difficult to solve in general. We transform and relax it into a convex problem and apply flow-shop scheduling techniques to address it. Furthermore, an alternative algorithm is developed to set the initial point closer to the optimal solution. Simulation results show that the total energy consumption of the UAV can be effectively reduced by the proposed scheme compared with the conventional systems.**

***Index Terms*—Internet of things, unmanned aerial vehicle (UAV), mobile edge computing (MEC), wireless power transfer (WPT), resources allocation, flow-shop scheduling.**

I. Introduction

INTERNET of things devices (IoTDs), such as smart home, wearable, traffic and other monitoring devices, spring up in our daily life [1]. However, some kinds of the IoTDs (e.g., security cameras, meter collection devices, temperature sensors) normally have very limited or even no computation capability due to their limited physical sizes. Therefore, it is difficult for these devices to process its collected data and respond to the environmental or the other changes intelligently. Moreover, in some areas, e.g., farming, the IoTDs may be too far from the energy source. Thus, it is difficult to charge them conveniently and cost-effectively.

Fortunately, the mobile edge computing (MEC) and the wireless power transfer (WPT) provide the solution to the above problems. As for the computing part, the MEC brings the computing resources closer to the users [2], [3]. Nevertheless, the remote IoTDs, which are for monitoring purpose, may be too far from the wireless access point or the edge cloud infrastructure. In these cases, it is very difficult for the IoTDs to enjoy the benefit provided by the MEC. Moreover, it may not be cost-effective to install the whole infrastructure to those remote devices as well. As for the charging part, the WPT is a promising technology to provide the cost-effective energy supplies to the low-power Internet of Things (IoT) wireless networks [4]. With the help of Energy Harvesting (EH) technology, the IoTDs can harvest the wireless signal to power themself. However, the severe propagation loss of the radio frequency (RF) signals over long distance reduces the performance of the practical WPT and EH systems.

With the increasing popularity of the UAV wide range applications (e.g., communication platforms, precision agriculture, surveillance and monitoring, cargo delivery), the UAV-assisted systems have drawn significant research interests recently [5], [6]. Particularly, the low-altitude UAV can serve as base stations (BSs) or relays to enhance the performance of the communication systems. Furthermore, different from the fixed location BSs, the UAV can exploit its mobility to fly closer to each user. Thus, the line-of-sight (LoS) links and better communication channels can be established [7].

By deploying the edge computing-enabled UAV to the remote IoTDs, we can not only save the cost of the physical infrastructure, but can also provide the computing resources on demand [8]. Different from the previous systems [9], [10], the proposed system uses the UAV as a flexible computing platform. Also, compared with the conventional WPT systems, the UAV can fly close enough to the IoTDs from one place to another [11], which can enlarge the WPT service coverage range and enhance the power transmission efficiency at the same time [12].

In this paper, we consider the UAV as a moving energy source to power the IoTDs, as illustrated in Fig.1. Further-

The work in the paper was partly funded by Natural Science Foundation of China (Grant No. 61620106011, 61572389), Zhongshan City Project (Grant No. 180809162197874). *(*Corresponding author: Kun Yang.)*

Y. Du and Y. Zhao are with the School of Information and Communication Engineering, University of Electronic Science and Technology of China, Chengdu 611731, China (e-mail: yaodu@std.uestc.edu.cn, yzzhao@std.uestc.edu.cn).

K. Yang is with the School of Computer Science and Electronic Engineering, University of Essex, CO4 3SQ Colchester, U.K., and also with the School of Information and Communication Engineering, University of Electronic Science and Technology of China, Chengdu 611731, China (e-mail: kunyang@essex.ac.uk).

K. Wang is with the Department of Computer and Information Sciences, Northumbria University, K. Wang is with the Department of Computer and Information Sciences, Northumbria University, Newcastle NE1 8ST, U.K., (e-mail: kezhi.wang@northumbria.ac.uk).

G. Zhang is with the School of Computer Science and Technology, China University of Mining and Technology, Xuzhou 221116, China (e-mail: gpzhang@cumt.edu.cn).

D. Chen is with the School of Electronic Information Engineering, University of Electronic Science and Technology of China, Zhongshan Institute, Zhongshan 528400, China (e-mail: chendwzsc@zsc.edu.cn).

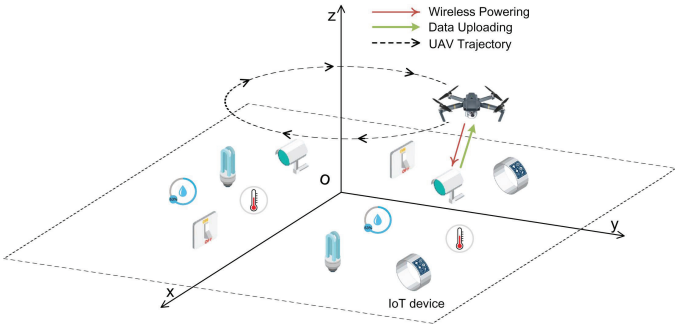

Fig. 1. The proposed UAV-enabled wirelessly-powered MEC system for IoT devices

more, the single antenna and central computing unit are installed on the UAV. In one UAV flying cycle, as depicted in Fig.1, the UAV flies above the IoTDs from one place to another and then flies back to the initial location.

In the above scenario, the UAV has several kinds of multi-user tasks (e.g., WPT, communication and computation tasks) to complete in one flying mission. However, the conventional working pattern of the UAV-assisted system contains only one workflow to complete all the tasks [13], which is inefficient compared with the multi-workflow system [14]. Motivated by the above reasons, a new TDMA based workflow structure for the UAV is studied in this paper. In order to minimize the UAV energy consumption, the IoTDs association, computing resources allocation, UAV hovering time, wireless powering duration, the uplink data rate and the services sequence of the IoTDs are jointly optimized based on the structure of the proposed multi-workflow system.

To the best of the authors' knowledge, this is the first work that considers multi-workflow structure in this type of UAV-assisted systems. Our contributions are as follows.

- In order to prolong UAV's serving time and enhance the energy efficiency, we design a TDMA based workflow model for the UAV-assisted system. The workflow model has multiple workflows and allows parallel operations of different IoTDs;
- We formulate the UAV energy minimization problem based on the proposed workflow structure. The problem is solved by the block-coordinate descent method (BCD);
- Relying on the Lagrange dual method, we achieve the closed-form optimal solution of the computing resources allocation problem for all IoTDs;
- By utilizing flow-shop scheduling techniques, we solve the formulated flow-shop problem and obtain the optimal IoTDs sequence.

The rest of this paper is organized as follows. Section II surveys the related works on the UAV-enabled MEC and WPT system, and also on the resources allocation and mobility design of the UAV. The Section III introduces the proposed system model and the UAV energy minimization problem, whereas in Section IV and V, we investigate the problem in single workflow and multi-workflow system, respectively. The efficient algorithms are proposed to minimize the UAV energy consumption. Section VI provides the simulation results. Finally, we conclude the paper in Section VII.

TABLE I
List of The Key Symbols

Parameter	Definition
N	The number of the IoTDs
M	The number of the hovering locations
H	The altitude of the UAV
(X_j, Y_j, H)	The j-th hovering place of the UAV
$(x_i, y_i, 0)$	The position of each i-th IoTD
D_i	The amount of transmitted data from each i-th IoTD to the UAV
F_i	The total number of CPU cycles that the UAV costs to process each i-th IoTD data
a_{ij}	The IoTDs association
f_{ij}	The computing resources allocated to each i-th IoTD in each j-th UAV hovering place
t_{ij}^{w}	The WPT time for each i-th IoTD in each j-th UAV hovering place
h_{ij}	The channel power gain of each i-th IoTD in each j-th time slot
t_i^{qos}	The QoS requirement of each i-th IoTD
κ_i	The effective switched capacitance
v_i	The WPT power conversion efficiency at each i-th IoTD
t_{ij}^{u}	The data uploading time for each i-th IoTD in each j-th UAV hovering place
t_{ij}^{c}	The task computing time for each i-th IoTD in each j-th UAV hovering place
T_j	Each j-th UAV hovering time
S_j	The services sequence of the IoTDs in each j-th UAV hovering place
$\mathbb{S}_j$	The set of different IoTDs permutations in each j-th UAV hovering place
K_j	The number of the IoTDs served in each j-th UAV hovering location
$\mathcal{K}_j$	The set of the IoTDs which select the j-th UAV hovering place to upload their data
s_{kj}^{w}	The WPT start time of the k-th service flow in each j-th UAV hovering place
s_{kj}^{u}	The uploading start time of the k-th service flow in each j-th UAV hovering place
s_{kj}^{c}	The computing start time of the k-th service flow in each j-th UAV hovering place
s_{kj}^{tf}	The transferring stage start time of the k-th service flow in each j-th UAV hovering place
c_{kj}^{w}	The WPT completion time of the k-th service flow in each j-th UAV hovering place
c_{kj}^{u}	The uploading completion time of the k-th service flow in each j-th UAV hovering place
c_{kj}^{c}	The computing completion time of the k-th service flow in each j-th UAV hovering place
c_{kj}^{tf}	The transferring stage completion time of the k-th service flow in each j-th UAV hovering place
φ	The optimization weight of the battery consumption
ϕ	The optimization weight of the solar energy consumption
p_i	The power of each i-th IoTD antennas
P_{uav}^{W}	The power of the UAV WPT antennas
P_{uav}^{H}	The hovering power of the UAV

II. Related Works

As mentioned above, the use of UAV to improve the performance of the wireless networks has attracted considerable attention recently. To be more specific, the information collection and data fusion scenario is considered in [15], where the RF signal is applied to UAV position estimation and collision avoidance. The work in [16] demonstrates how UAV can be used to promptly construct a Device-to-Device (D2D) enabled network [17], which is agile enough to support the content sharing and delivery in the network. Furthermore, the UAV

can be used as a relay node to improve the communication performance. In order to avoid heavily jamming or interfering in vehicular ad hoc networks, the authors in [18] propose an UAV anti-jamming relay strategy based on reinforcement learning. In [19], the UAV detects the location information of the IoT nodes and relay the collected information to the cloud in order to generate the physical and logical topology of the large-scale IoT system. The work in [20] employs Age-of-information (AoI) as a metric to quantify the freshness of information at the destination node. In order to minimize the average peak AoI, the authors optimize the UAV's flight trajectory as well as energy and service time allocations for packet transmissions. In [21], an efficient time-slot allocation for enhancing the frequency resources utilization is proposed, where the target field is divided into virtual hexagonal cells. Moreover, the authors in [22] consider the access selection and resources allocation in UAV assisted IoT communication networks, where a hierarchical game framework is presented to solve the joint optimization problem. In addition, in order to enable reliable IoT uplink communications, the work in [23] introduces a novel framework by jointly optimizing the 3D placement and the mobility of the UAV, device-UAV association, and uplink power control.

Compared with cloud computing server, the edge cloud computing server is closer to the mobile users but has less computing resources [1], [24]. The main requirement of such a system is having a low service delay, which would correspond to a high Quality of Service (QoS) [25]. Therefore, the work in [26] focuses on minimizing the service delay by virtual machine resources management and transmission power controlling. However, as the number of clients and devices grows, the service must also increase its scalability in order to guarantee a latency limitation and quality threshold. Thus, the edge servers activation scheme for scalable MEC is proposed in [27]. Furthermore, the UAV can play an important role in the mobile edge computing system. The work in [8] and [28] consider the UAV as an edge server which provides the offloading opportunities [24] to multiple static mobile devices. The authors in [29] apply the UAV-enabled MEC to the location based social network. They design an accurate location-based recommendation system where the UAV carries out adaptive recommendation in a distributed manner so as to reduce computing and traffic load.

In addition, the far-field WPT [30] via RF radiation is able to operate over a much longer range compared with the near-field WPT based on inductive coupling or magnetic resonant coupling [12]. UAV-enabled WPT has recently emerged as a promising solution to prolong the lifetime of low-power sensors and IoT devices. Moreover, the energy harvesting cooperative wireless sensor networks (WSNs) for IoT systems are investigated in [31]. The authors propose a new type of WSNs that integrates EH and WPT technologies to provide the continuous and controllable energy supply. Furthermore, if the energy receiver node is far from the energy transmitter, the far-apart nodes can hardly harvest the energy and they require more energy for the same throughput as near-apart nodes due to distance-dependent signal attenuation. In order to solve the above problem, the authors in [32] use the UAV as a mobile energy transmitter and propose a weighted harvest-then-transmit protocol. The work in [33] considers the multi-user wireless power transfer and maximizes the uplink throughput among all ground users over a finite UAV's flight period. Moreover, the maximization of the sum energy received by all energy receivers is studied in [12]. The proposed UAV trajectory solution implies that the UAV should hover over a set of fixed locations with optimal hovering time. However, the UAV hovering time can be further reduced in order to minimize the UAV energy consumption. Therefore, a new model is required for the UAV hovering design in such networks, which is discussed in the following section.

III. System Model

A. Working Pattern Model

Without loss of generality, a three-dimensional (3D) Euclidean coordinate is adopted. We define O as the geometric center of all the IoTDs. The location of each i-th IoTD is given as $(x_i, y_i, 0)$, $i \in \mathcal{N} = \{1, 2, \dots, N\}$. Also, we assume that the UAV flies above the target area and hovers at M given locations in its one working cycle, and the location of the UAV is denoted by (X_j, Y_j, H), $j \in \mathcal{M} = \{1, 2, \dots, M\}$. Each j-th hovering duration lasts the time of T_j seconds, where each IoTD selects one time interval to upload their data and waits for the executions and instructions from the UAV. We assume the hovering locations are chosen wisely to cover all IoTDs, therefore each IoTD can choose at least one hovering location to upload its collected data.

In our proposed system, each IoTD could choose only one UAV hovering location to upload its data while in UAV's one hovering location, it can serve more than one IoTD. We define a_{ij} as the IoTDs association, where $a_{ij} = 1$ means the i-th IoTD chooses the j-th UAV hovering location to upload data, otherwise, $a_{ij} = 0$. Thus, one can have

$$\sum_{j=1}^{M} a_{ij} = 1, \forall i \in \mathcal{N}, \forall j \in \mathcal{M} \tag{1}$$

Also, one can have

$$a_{ij} = \{0,1\}, \forall i \in \mathcal{N}, \forall j \in \mathcal{M} \tag{2}$$

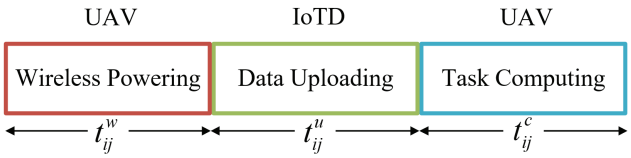

Fig. 2. Three stages of one service flow

Furthermore, as illustrated in Fig. 2, the structure of one service flow consists of three stages, namely the UAV wireless powering stage during which the UAV transfers energy, the IoTD data uploading stage during which the IoTD transmits the collected data and the UAV task computing stage during which the UAV computes the collected data. The three stages last the time of t_{ij}^{w}, t_{ij}^{u} and t_{ij}^{c}, respectively.

To be more specific, the working pattern of the UAV-enabled MEC system is described as follows:

- *Service Initialization*: The UAV flies to the specific location and hovering, then it sends signal to a IoTD to switch its working mode to the EH mode in order to harvest the RF energy, then the IoTD will be ready to be charged by the UAV;
- *Wireless Powering*: The UAV transfers energy to the IoTD via WPT technology. Note that the other remote IoTDs are in their data collecting mode, in which the IoTD cannot be charged by the UAV. Moreover, the remote IoTDs are too far from the UAV to harvest wireless energy;
- *Mobile Edge Computing*: The IoTD uploads its collected data to the UAV. The UAV may apply the trained machine learning model to process the transmitted data and then return the instructions to the IoTDs. According to the computations in UAV, the instructions to the IoTDs may include adjustment of their data collection frequencies or the working patterns.

B. The TDMA Based Workflow Model

In the proposed UAV-enabled MEC system, we consider the returned instructions only cost a small amount of data and therefore can be ignored from our model. In the conventional MEC system, the access point, i.e., the UAV, usually has only one workflow. Therefore, each device should wait until the former device completes its last operation, which results in long services makespan, i.e., the UAV hovering time. Thus, the considerable energy loss happens. Different from the previous UAV-enabled MEC system [13], the TDMA based workflow allows parallel transmissions and executions for different devices, as depicted in Fig. 3. Thus, the hovering time of the UAV is minimized and the QoS of each IoTD is guaranteed at the same time.

Moreover, in each j-th UAV hovering location, we define T_j as each j-th UAV hovering time. Let S_j denote the services sequence of the IoTDs, which select the j-th UAV hovering location to upload their collected data.

Furthermore, in Fig. 3 (a), we illustrate an example of many random service flows without optimization, which means the services flow in Fig. 3 (a) is poorly ordered. In this case, the UAV will follow the poorly ordered workflows to serve the IoTDs. Thus, there is some gap time between the first data uploading time and first task computing time in Fig. 3 (a). Despite all of these, one can notice that the proposed multi-workflow structure can still save more hovering time compared with the single workflow structure.

For brevity and easily understanding, in Fig. 3 (b), we illustrate the optimized service flows of four IoTDs. Note that once we get the optimal duration of each stage, the optimal IoTDs' services sequence S_j^* can be obtained by our optimization. The detailed optimization will be introduced in Section V. Next, we give the mathematical model of the proposed TDMA based workflow structure and we optimize the workflows in order to obtain the optimal hovering time T_j^*.

In addition, the structure of the proposed workflow can be modeled as the standard three-stage flow-shop model [14]. Note that the flow-shop model is applied in each j-th hovering place of one UAV.

For simplicity, we define K_j as the number of the IoTDs served in each j-th UAV hovering location and $\mathcal{K}_j$ is the IoTDs set in which the IoTDs select the j-th UAV hovering place to upload their data. We define "!" as the factorial operation. Then $\mathbb{S}_j$ denotes the set of the $K_j!$ (the factorial of K_j) different permutations in $\mathcal{K}_j$.

We introduce an example as follows for easily understanding: assume there are three devices (i.e., IoTD-1, IoTD-2 and IoTD-3) in the first UAV hovering place. Then $\mathbb{S}_1$ is the set of 3! different permutations, which is $\{123, 132, 213, 231, 312, 321\}$. Thus, one can have

$$S_j \in \mathbb{S}_j, \forall j \in \mathcal{M} \tag{3}$$

Different from the index i of IoTDs, we define k as the index of the workflow sequences in one UAV hovering place. In each j-th UAV hovering place, as depicted in Fig. 3, let $\boldsymbol{s}_{kj} = [s_{kj}^w, s_{kj}^u, s_{kj}^c]$ denote the starting time vector of each operation (i.e., wireless powering, data transmission and processing, respectively) in the k-th service flow. Let $\boldsymbol{t}_{kj} = [t_{kj}^w, t_{kj}^c, t_{kj}^u]$ denote the duration vector of three service stages in k-th workflow. Let $\boldsymbol{c}_{kj} = [c_{kj}^w, c_{kj}^u, c_{kj}^c]$ denote the completion time vector of the operation corresponding to $\boldsymbol{s}_{kj}$, where $k \in \mathcal{K}_j$. Note that each of the three stages cannot be interrupted, thus

$$\boldsymbol{s}_{kj} + \boldsymbol{t}_{kj} = \boldsymbol{c}_{kj}, k \in \mathcal{K}_j, \forall j \in \mathcal{M} \tag{4}$$

In the proposed system model, the wireless powering, the data transmission and the task execution of each k-th service flow are operated sequentially. As illustrated in Fig. 3, the data uploading stage is after the wireless powering stage and the task computing stage is after the data uploading stage, therefore

$$\begin{cases} s_{kj}^w \geq 0 \\ s_{kj}^u \geq c_{kj}^w \\ s_{kj}^c \geq c_{kj}^u \end{cases}, k \in \mathcal{K}_j, \forall j \in \mathcal{M} \tag{5}$$

Moreover, there are at most one IoTD being served at one time in each workflow, which means the k-th stage is after the (k-1)-th stage. Thus

$$\begin{cases} s_{kj}^w \geq c_{k-1,j}^w \\ s_{kj}^u \geq c_{k-1,j}^u \\ s_{kj}^c \geq c_{k-1,j}^c \end{cases}, k \in \mathcal{K}_j, \forall j \in \mathcal{M} \tag{6}$$

Notice that the WPT power of the UAV antenna is usually far greater than the communication transmit power of the IoTD antenna [34], [35]. If the IoTD transmits its data and the UAV transfers wireless energy at the same time, the communication signal will be drowned out by the WPT signal. Therefore, the k-th WPT operation should be performed after the (k-1)-th uploading operation. One can have

$$s_{kj}^w \geq c_{k-1,j}^u, k \in \mathcal{K}_j, \forall j \in \mathcal{M} \tag{7}$$

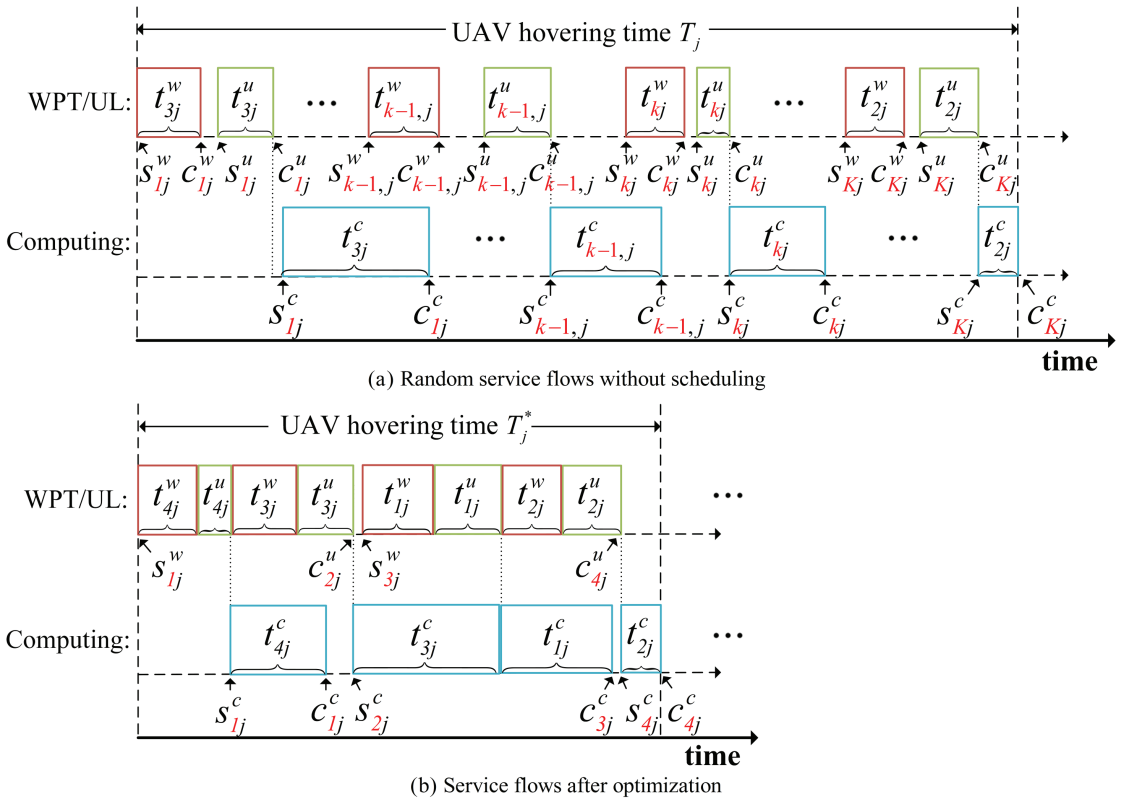

(a) Random service flows without scheduling

(b) Service flows after optimization

Fig. 3. The proposed TDMA based workflow

C. Task Model

We define D_i as the amount of the transmitted data from each i-th IoTD to the UAV and F_i is the total number of the CPU cycles that the UAV applies to process the data. Thus, one can express the task from each i-th IoTD as $(D_i, F_i, t_i^{qos}), \forall i \in \mathcal{N}$, where the F_i can be obtained by using the approaches provided in [36].

We define B as the channel bandwidth and p_i as the transmitting power of each i-th IoTD, σ^2 as the noise power at the receiver of each IoTD and $d_{ij} = \sqrt{(X_j - x_i)^2 + (Y_j - y_i)^2 + H^2}$ as the distance between each i-th IoTD and the UAV in j-th hovering place. Then the channel power gain [8] of the i-th IoTD in the j-th hovering place is

$$h_{ij} = \frac{h_0}{d_{ij}^2} \tag{8}$$

where the h_0 represents the received power at the reference distance d_0 = 1 m. In each j-th hovering place, the achievable uplink data rate r_{ij} for each i-th IoTD in the j-th hovering location is given by

$$r_{ij} = a_{ij} B \log_2 \left(1 + \frac{p_i h_{ij}}{\sigma^2}\right), \forall i \in \mathcal{N}, \forall j \in \mathcal{M} \tag{9}$$

The time used to send the data from each i-th IoTD to the UAV in its j-th hovering place is

$$t_{ij}^u = \frac{D_i}{r_{ij}}, \forall i \in \mathcal{N}, \forall j \in \mathcal{M} \tag{10}$$

We define f_{ij} as the actual computing resources allocated by the UAV. In each j-th hovering place, the required time for data processing at the UAV is

$$t_{ij}^c = \frac{F_i}{f_{ij}}, \forall i \in \mathcal{N}, \forall j \in \mathcal{M} \tag{11}$$

In the proposed system, the UAV processes the IoTDs collected data one by one. Thus, one can have

$$0 \le f_{ij} \le f_{max}, \forall i \in \mathcal{N}, \forall j \in \mathcal{M} \tag{12}$$

where f_{max} is the maximal UAV computation resource.

Also, the UAV is required to provide sufficient computing resources for each IoTD

$$\sum_{j=1}^{M} a_{ij} f_{ij} t_{ij}^c \ge F_i, \forall i \in \mathcal{N}, \forall j \in \mathcal{M} \tag{13}$$

We assume all the wireless powering, data uploading and processing for each IoTD have to be completed in t_i^{qos}, then one can have

$$a_{ij}(c_{ij}^c - s_{ij}^w) \le t_i^{qos}, \forall i \in \mathcal{N}, \forall j \in \mathcal{M} \tag{14}$$

D. UAV Energy Consumption Model

The energy consumption model of the UAV consists of three parts, i.e., the computing energy, the wireless powering energy and the hovering energy. We assume the computing operation and the WPT operation are powered by the UAV battery and the UAV rotor wings are powered by solar panels [37]. Therefore, the two types of energy consumption are optimized

with different weight in the formulated problem of the next Section III.

We define the computing energy consumption of the UAV for each task as $\kappa_i(f_{ij})^{\gamma_i}t^c_{ij}$, where $\kappa_i \geq 0$ is the effective switched capacitance and γ_i is the positive constant. To match the realistic measurements, we set $\kappa_i = 10^{-26}$ and γ_i = 3 [38] here.

The WPT power conversion efficiency at each i-th IoTD is defined as v_i. At each j-th UAV hovering location, the total energy harvested by each i-th IoTD can be written as E^W_{ij}, which should be more than the uploading energy each IoTD consumes. Thus, one can have

$$E^W_{ij} = v_i h_{ij} P^W_{uav} t^w_{ij} \geq p_i t^u_{ij}, \forall i \in \mathcal{N}, \forall j \in \mathcal{M} \tag{15}$$

We define P^H_{uav} as the fixed UAV hovering power consumption, P^W_{uav} as the fixed power of the UAV WPT antennas, $\boldsymbol{\varphi}$ and $\boldsymbol{\phi}$ as the optimization weights. The hovering energy of the UAV in each j-th hovering location is written as E^H_j. Thus, the total energy consumption (denoted by E) of the UAV can be given as

$$\begin{aligned} E &= \boldsymbol{\varphi}(E^C + E^W) + \boldsymbol{\phi}E^H && \text{(16a)} \\ &= \boldsymbol{\varphi}\sum_{i=1}^{N}\sum_{j=1}^{M} a_{ij}\kappa_i(f_{ij})^{\gamma_i}t^c_{ij} + \boldsymbol{\varphi}\sum_{i=1}^{N}\sum_{j=1}^{M} a_{ij}E^W_{ij} \\ &\quad + \boldsymbol{\phi}\sum_{j=1}^{M} E^H_j && \text{(16b)} \\ &= \boldsymbol{\varphi}\sum_{i=1}^{N}\sum_{j=1}^{M} \kappa_i F_i a_{ij}(f_{ij})^2 + \boldsymbol{\varphi}\sum_{i=1}^{N}\sum_{j=1}^{M} a_{ij}v_i h_{ij}P^W_{uav}t^w_{ij} \\ &\quad + \boldsymbol{\phi}P^H_{uav}\sum_{j=1}^{M} T_j && \text{(16c)} \end{aligned}$$

E. Problem Formulation

Assume that the locations of the IoTDs and the UAV's hovering places are fixed and known [39]. Let $\boldsymbol{A} = \{a_{ij}, \forall i \in \mathcal{N}, \forall j \in \mathcal{M}\}$, $\boldsymbol{F} = \{f_{ij}, \forall i \in \mathcal{N}, \forall j \in \mathcal{M}\}$, $\boldsymbol{r} = \{r_{ij}, \forall i \in \mathcal{N}, \forall j \in \mathcal{M}\}$, $\boldsymbol{t} = \{T_j, t^w_{ij}, t^u_{ij}, t^c_{ij}, \forall i \in \mathcal{N}, \forall j \in \mathcal{M}\}$, $\boldsymbol{S} = \{S_j, \boldsymbol{s}_{kj}, \boldsymbol{c}_{kj}, k \in \mathcal{K}_j, \forall j \in \mathcal{M}\}$. In the optimization problem below, we aim to jointly optimize the IoTDs association (i.e., $\boldsymbol{A}$), the computing resources allocation (i.e., $\boldsymbol{F}$), the uplink data rate (i.e., $\boldsymbol{r}$), and the UAV hovering durations (i.e., $\boldsymbol{t}$) including different services time, and the services sequence of the IoTDs (i.e., $\boldsymbol{S}$) at each UAV hovering location. Then, the optimization problem is formulated as

$$\begin{aligned} \mathcal{P}1: \underset{\boldsymbol{A},\,\boldsymbol{F},\,\boldsymbol{r},\,\boldsymbol{t},\,\boldsymbol{S}}{\text{minimize}}\ & \boldsymbol{\varphi}(E^C + E^W) + \boldsymbol{\phi}E^H \\ \text{s.t. } & \text{(1)-(10), (9)-(15)} \end{aligned} \tag{17}$$

The original $\mathcal{P}1$ is difficult to solve due to the following reasons. Firstly, the IoTDs association variables $\boldsymbol{A}$ are binary, therefore constraint (1),(2),(13),(14) and (15) involve integer constraints; Secondly, even with the fixed $\boldsymbol{A}$, $\mathcal{P}1$ is still a non-convex problem because of the non-convex constraints (6), (7) and (14); Thirdly, to obtain the optimal UAV hovering time T^*_j, one should solve the three stages flow-shop problem, which is NP-hard [14]. Therefore, the original $\mathcal{P}1$ is a mixed-integer non-convex problem, which is difficult to be optimally solved in general.

By observing the interrelationship between the optimization variables, we find that the distance between the UAV and each IoTD is directly decided by the IoTD association a_{ij}. One can notice that the data rate r_{ij} is determined by the distance d_{ij} according to the equations (8) and (9). Therefore the data rate r_{ij} is determined by a_{ij}. Given any r_{ij}, the t^u_{ij} can be achieved by equation (10). Moreover, given any f_{ij}, the t^c_{ij} is determined by (11). Therefore, in order to make $\mathcal{P}1$ tractable, we can transform it equivalently as follows

$$\begin{aligned} \underset{\boldsymbol{A},\,\boldsymbol{F},\,\boldsymbol{\tau},\,\boldsymbol{T},\,\boldsymbol{S}}{\text{minimize}}\ & \boldsymbol{\varphi}(E^C + E^W) + \boldsymbol{\phi}E^H \\ \text{s.t. } & \text{(1)-(7), (12)-(15)} \end{aligned} \tag{18}$$

where we redefine $\boldsymbol{\tau} = \{t^w_{ij}, \forall i \in \mathcal{N}, \forall j \in \mathcal{M}\}$ as the wireless powering duration and $\boldsymbol{T} = \{T_j, \forall j \in \mathcal{M}\}$ as the UAV hovering time.

Next, we investigate both single workflow system and multi-workflow system optimization in Section IV and V, respectively. The single workflow system is relatively simple and has been widely applied in UAV-enabled systems [13]. Therefore, we give the single workflow system optimization for the current widely applied single workflow system. Note that the multi-workflow system is an updated version of the single workflow UAV-enabled system. In addition, compared with the single workflow system, the proposed multi-workflow system is more energy efficient, thus we propose the novel multi-workflow system optimization in order to reduce the UAV energy consumption.

IV. UAV Energy Consumption Minimization in the Single Workflow System

In this section, we consider the UAV energy minimization in the Single Workflow system. One can see that the UAV energy consumption minimization problem in the single workflow system is a special case of $\mathcal{P}1$, in which the services sequence of the IoTDs (i.e., $\boldsymbol{S}$) is irrelevant to the hovering time (i.e., $\boldsymbol{T}$). Therefore, $\boldsymbol{S}$ is irrelevant to the UAV energy consumption and there is no need to optimize $\boldsymbol{S}$. Thus, we reformulate $\mathcal{P}1$ as

$$\underset{\boldsymbol{A},\,\boldsymbol{F},\,\boldsymbol{\tau},\,\boldsymbol{T}}{\text{minimize}}\ \boldsymbol{\varphi}(E^C + E^W) + \boldsymbol{\phi}E^H \tag{19a}$$

$$\text{s.t. } a_{ij} = \{0,1\}, \forall i \in \mathcal{N}, \forall j \in \mathcal{M} \tag{19b}$$

$$\sum_{j=1}^{M} a_{ij} = 1, \forall i \in \mathcal{N}, \forall j \in \mathcal{M} \tag{19c}$$

$$0 \leq f_{ij} \leq f_{max}, \forall i \in \mathcal{N}, \forall j \in \mathcal{M} \tag{19d}$$

$$v_i h_{ij} P^W_{uav} t^w_{ij} \geq p_i t^u_{ij}, \forall i \in \mathcal{N}, \forall j \in \mathcal{M} \tag{19e}$$

$$a_{ij}(t^w_{ij} + t^u_{ij} + t^c_{ij}) \leq t^{qos}_i, \forall i \in \mathcal{N}, \forall j \in \mathcal{M} \tag{19f}$$

$$T_j \geq \sum_{i=1}^{N} a_{ij}(t^w_{ij} + t^u_{ij} + t^c_{ij}), \forall i \in \mathcal{N}, \forall j \in \mathcal{M} \tag{19g}$$

Notice that problem (19) is a mixed-integer non-convex problem, which is difficult to find the optimal solution. We next transform problem (19) into a more tractable problem, and we also develop an iterative algorithm to find the sub-optimal solution.

Theorem 1. *The optimal hovering time of the single workflow UAV is*

$$T_j^* = \sum_{i=1}^{N} a_{ij}(t_{ij}^w + t_{ij}^u + t_{ij}^c),\ \forall j \in \mathcal{M} \tag{20}$$

Proof. Please refer to Appendix A. □

In the proposed system, the wireless powering energy from the UAV is used for the IoTDs data uploading. One can see that, constraint (19f) is the upper bound of t_{ij}^w and constraint (19e) is the lower bound of t_{ij}^w.

Theorem 2. *The optimal UAV WPT time is*

$$t_{ij}^{w*} = \frac{p_i t_{ij}^u}{v_i h_{ij} P_{uav}^W},\ \forall i \in \mathcal{N},\ \forall j \in \mathcal{M} \tag{21}$$

Proof. Please refer to Appendix B. □

According to Theorem 1 and Theorem 2, we relax and transform problem (19) into problem (22).

$$\underset{\boldsymbol{A},\,\boldsymbol{F}}{\text{minimize}}\ \boldsymbol{\varphi}\sum_{i=1}^{N}\sum_{j=1}^{M}\kappa_i F_i a_{ij}(f_{ij})^2 + \boldsymbol{\varphi}\sum_{i=1}^{N}\sum_{j=1}^{M} a_{ij} p_i t_{ij}^u + \boldsymbol{\phi} P_{uav}^H \sum_{i=1}^{N}\sum_{j=1}^{M} a_{ij}(p_i t_{ij}^u / v_i h_{ij} P_{uav}^W + t_{ij}^u + F_i/f_{ij}) \tag{22a}$$

$$\text{s.t. } 0 \le a_{ij} \le 1,\ \forall i \in \mathcal{N},\ \forall j \in \mathcal{M} \tag{22b}$$

$$\sum_{j=1}^{M} a_{ij} = 1,\ \forall i \in \mathcal{N},\ \forall j \in \mathcal{M} \tag{22c}$$

$$0 \le f_{ij} \le f_{max},\ \forall i \in \mathcal{N},\ \forall j \in \mathcal{M} \tag{22d}$$

$$a_{ij}(t_{ij}^w + t_{ij}^u + F_i/f_{ij}) \le t_i^{qos},\ \forall i \in \mathcal{N},\ \forall j \in \mathcal{M} \tag{22e}$$

In order to minimize the energy consumption of the UAV and guarantee the QoS of each IoTD, the UAV should allocate less than its full computing capacity to each IoTD. Given any IoTDs association $\boldsymbol{A}$, problem (22) is reformulated as follows

$$\underset{\boldsymbol{F}}{\text{minimize}}\ \sum_{i=1}^{N}\sum_{j=1}^{M}(\boldsymbol{\varphi}\kappa_i F_i a_{ij} {f_{ij}}^2 + \frac{\boldsymbol{\phi} P_{uav}^H a_{ij} F_i}{f_{ij}}) \tag{23a}$$

$$\text{s.t. } f_{ij}^l \le f_{ij} \le f_{max} \tag{23b}$$

Theorem 3. *Problem (23) is a convex problem and the optimal solution f_{ij}^* to the computing resources allocation is*

$$f_{ij}^* = \begin{cases} f_{ij}^l & \sqrt[3]{\frac{\phi P_{uav}^H}{2\varphi\kappa_i}} < f_{ij}^l \\ \sqrt[3]{\frac{\phi P_{uav}^H}{2\varphi\kappa_i}} & f_{ij}^l \le \sqrt[3]{\frac{\phi P_{uav}^H}{2\varphi\kappa_i}} \le f_{max} \\ f_{max} & \sqrt[3]{\frac{\phi P_{uav}^H}{2\varphi\kappa_i}} > f_{max} \end{cases} \tag{24}$$

Note that we define the lower bound of f_{ij} as $f_{ij}^l = \frac{a_{ij}F_i}{t_i^{qos} - a_{ij}(t_{ij}^w + t_{ij}^u)}$.

Proof. Please refer to Appendix C. □

In order to minimize the energy consumption of the UAV, each IoTD should choose an optimum UAV hovering place to upload data. For any given computing resources allocation, the IoTDs association problem is

$$\underset{\boldsymbol{A}}{\text{minimize}}\ \sum_{i=1}^{N}\sum_{j=1}^{M}[\boldsymbol{\varphi}(\kappa_i F_i f_{ij}^2 + p_i t_{ij}^u) + \boldsymbol{\phi} P_{uav}^H (t_{ij}^w + t_{ij}^u + t_{ij}^c)] a_{ij} \tag{25a}$$

$$\text{s.t. } 0 \le a_{ij} \le 1,\ \forall i \in \mathcal{N},\ \forall j \in \mathcal{M} \tag{25b}$$

$$\sum_{j=1}^{M} a_{ij} = 1,\ \forall i \in \mathcal{N},\ \forall j \in \mathcal{M} \tag{25c}$$

Notice that problem (25) is a standard linear programming (LP) problem, which can be solved by the well established optimization toolbox, e.g., CVX [40] optimally and efficiently. Furthermore, according to the structure of problem (25), the solution to problem (25) is binary. Thus, there is no need to reconstruct a binary solution to the original problem (19). Next we develop an iterative algorithm to solve problem (22).

Algorithm 1 The proposed iterative algorithm for problem (19)

1: Obtain the optimal wireless powering duration $\boldsymbol{\tau}^*$ by using eq. (21).
2: **Initialize:** $\boldsymbol{A}^0$ and let $r = 0$;
3: **Repeat:**
4: For given $\boldsymbol{A}^r$, use equation (24) to obtain the optimal solution denoted as $\boldsymbol{F}^{r+1}$;
5: For given $\boldsymbol{F}^{r+1}$, use CVX tool box to obtain the optimal solution denoted as $\boldsymbol{A}^{r+1}$;
6: Use equation (20) to obtain the optimal solution denoted as $\boldsymbol{T}^{r+1}$;
7: Update $r = r + 1$.
8: **Until:** The fractional decrease of E is below a threshold ϵ or a maximum number of iterations ($r_{\max}$) is reached;
9: **Return:** The optimal IoTDs association $\boldsymbol{A}^*$, computing resources allocation $\boldsymbol{F}^*$, UAV wireless powering duration $\boldsymbol{\tau}^*$ and UAV hovering durations $\boldsymbol{T}^*$.

Using the results above, the overall algorithm for computing the solution to problem (19) is summarized in Algorithm 1 with the computation complexity analyzed as follows. Given the solution accuracy of $\epsilon > 0$, the inner loop computation complexity is $\mathcal{O}((NM)^{3.5} log(1/\epsilon))$ in each iteration. This is because the IoTDs association is optimized by using the convex solver based on the interior-point method. As the BCD iterations are in the complexity of the order $log(1/\epsilon)$, the total computation complexity of Algorithm 1 is thus $\mathcal{O}((NM)^{3.5} log^2(1/\epsilon))$. In other words, Algorithm 1 can converge to an optimum solution with a polynomial time computational complexity.

V. UAV Energy Consumption Minimization in the Multi-Workflow System

In this section, we consider the UAV energy minimization in the Multi-Workflow system. We relax $\mathcal{P}1$ to a more tractable one. Also, an alternative algorithm is developed in this section to set the initial point closer to the optimal solution.

A. Problem Transformation and WPT Duration Optimization

Theorem 4. *According to Fig. 3 (b), the optimal UAV hovering time of the multi-workflow UAV is the differential time between the optimal wireless powering start time s_{1j}^{w*} and the optimal computing task completion time c_{Kj}^{c*}. Note that the optimal $s_{1j}^{w*}=0$. Therefore*

$$T_j^* = c_{Kj}^{c*},\ \forall j \in \mathcal{M} \tag{26}$$

To make $\mathcal{P}1$ more tractable and considering minimizing the serving time of each IoTD, we transform and relax the original $\mathcal{P}1$ into problem (27) as follows

$$\underset{\boldsymbol{A},\,\boldsymbol{F},\,\boldsymbol{\tau},\,\boldsymbol{S}}{\text{minimize}}\ \boldsymbol{\varphi}(E^C+E^W)+\boldsymbol{\phi}P_{uav}^H\sum_{j=1}^{M}c_{Kj}^c \tag{27a}$$

$$\text{s.t. } a_{ij}(t_{ij}^w+t_{ij}^u+t_{ij}^c)\le t_i^{qos},\ \forall i\in\mathcal{N},\ \forall j\in\mathcal{M} \tag{27b}$$

$$0\le a_{ij}\le 1,\ \forall i\in\mathcal{N},\ \forall j\in\mathcal{M} \tag{27c}$$

$$t_{ij}^w \ge \frac{p_i t_{ij}^u}{v_i h_{ij} P_{uav}^W},\ \forall i\in\mathcal{N},\ \forall j\in\mathcal{M} \tag{27d}$$

$$(1),(3),(12),(13)$$

Note that (27b) is obtained by relaxing (14) due to (4)-(7). According to Theorem 2, the optimal solution to the wireless powering duration t_{ij}^w is irrelevant with a_{ij}, f_{ij} nor S_j. Bring (21) into problem (27). With the fixed $\boldsymbol{t}_j^u$, one can have

$$\underset{\boldsymbol{A},\,\boldsymbol{F},\,\boldsymbol{S}}{\text{minimize}}\ \boldsymbol{\varphi}(E^C+E^W)+\boldsymbol{\phi}P_{uav}^H\sum_{j=1}^{M}c_{Kj}^c \tag{28}$$

$$\text{s.t. } (1),(3),(12),(13),(27b),(27c)$$

B. IoTDs Association

For any given computing resources allocation and services sequence $\{\boldsymbol{F},\,\boldsymbol{S}\}$, putting (21) into (28), the IoTDs association $\boldsymbol{A}$ of problem (28) can be optimized by solving the following problem

$$\underset{\boldsymbol{A}}{\text{minimize}}\ \sum_{i=1}^{N}\sum_{j=1}^{M}a_{ij}\Big[\kappa_i F_i(f_{ij})^2+\frac{p_i D_i}{B\log_2\left(1+\frac{p_i h_{ij}}{\sigma^2}\right)}\Big] \tag{29}$$

$$\text{s.t. } (1),\ (27c)$$

Notice that using (11), the constraint (13) can be replaced by the stricter constraint (1). Given any t_{ij}^w and f_{ij}, for each i-th IoTD, $a_{ij}=1$ if and only if $\kappa_i F_i(f_{ij})^2+p_i D_i/r_{ij}$ is minimal, otherwise $a_{ij}=0$. Then, problem (29) is a LP problem, which can be solved by the well established optimization toolbox, e.g., CVX [40] optimally and efficiently.

C. Computing Resources Allocation

For any given IoTDs association and services sequence $\{\boldsymbol{A},\,\boldsymbol{S}\}$, the computing resources allocation of problem (28) can be optimized by solving the following problem

$$\underset{\boldsymbol{F}}{\text{minimize}}\ \sum_{i=1}^{N}\sum_{j=1}^{M}\kappa_i F_i a_{ij}(f_{ij})^2 \tag{30a}$$

$$\text{s.t. } \frac{a_{ij}r_{ij}F_i}{t_i^{qos}r_{ij}-a_{ij}(D_i+t_{ij}^w r_{ij})}\le f_{ij}\le f_{max} \tag{30b}$$

$$(13)$$

Problem (30) is a convex problem and can be solved by applying convex optimization technique such as the interior-point method [41]. We next use the Lagrange dual method to obtain a well-structured solution.

The Lagrange multipliers associated with the constraints in (13) is given as $\boldsymbol{\mu}\triangleq\{\mu_i\ge 0,\forall i\in\mathcal{N}\}$. The partial Lagrangian function of problem (30) is

$$\begin{aligned}\boldsymbol{\mathcal{L}}(\boldsymbol{F},\boldsymbol{\mu}) =& \sum_{i=1}^{N}\sum_{j=1}^{M}\kappa_i F_i a_{ij}(f_{ij})^2\\ &+\sum_{i=1}^{N}\mu_i(F_i-\sum_{j=1}^{M}a_{ij}f_{ij}t_{ij}^c)\end{aligned} \tag{31}$$

Then the dual function of problem (30) can be given as

$$g(\boldsymbol{\mu})=\min_{\boldsymbol{F}}\ \boldsymbol{\mathcal{L}}(\boldsymbol{F},\boldsymbol{\mu}) \tag{32}$$

$$\text{s.t. (30b)}$$

Thus, the dual problem of problem (30) is

$$\max_{\boldsymbol{\mu}}\ g(\boldsymbol{\mu}) \tag{33a}$$

$$\text{s.t. } \mu_i\ge 0,\ \forall i\in\mathcal{N} \tag{33b}$$

Since problem (30) is convex and it also satisfies the Slater's condition, strong duality holds between problems (30) and (33). As a result, one can solve problem (30) by equivalently solving its dual problem (33).

1) Derivation of the Dual Function $g(\boldsymbol{\mu})$: Given any $\boldsymbol{\mu}$, we obtain $g(\boldsymbol{\mu})$ by solving problem (32). Note that problem (32) can be decomposed into the following $N\times M$ subproblems.

$$\min_{\boldsymbol{F}}\ \kappa_i F_i a_{ij}(f_{ij})^2\ -\ \mu_i a_{ij} f_{ij} t_{ij}^c \tag{34}$$

$$\text{s.t. (30b)}$$

According to the monotonicity of objective function, we present the optimal solution of problem (34) as

$$\begin{cases} f_{ij,a}^* = \dfrac{a_{ij}r_{ij}F_i}{t_i^{qos}r_{ij}-a_{ij}(D_i+t_{ij}^w r_{ij})}, \\ \qquad\qquad if\ 0\le\mu_{i,a}<b_{ij} & (35a)\\ f_{ij,b}^* = \dfrac{\mu_i t_{ij}^c}{2\kappa_i F_i},\ if\ b_{ij}\le\mu_{i,b}\le\dfrac{2\kappa_i F_i f_{\max}}{t_{ij}^c} & (35b)\\ f_{ij,c}^* = f_{\max},\ if\ \mu_{i,c}>\dfrac{2\kappa_i F_i f_{\max}}{t_{ij}^c} & (35c)\end{cases}$$

In eq. (35a)-(35c), we divide the optimal solution $\boldsymbol{F}^*$ as $f_{ij,a}^*$, $f_{ij,b}^*$ and $f_{ij,c}^*$, respectively, in accordance with the three

parts of $\boldsymbol{\mu}$'s defined domain in (35). Let $\mu_{i,a}$, $\mu_{i,b}$ and $\mu_{i,c}$ represent three different kinds of μ_i in (35) intervals. Also, we define $b_{ij} = \frac{2\kappa_i a_{ij} r_{ij} F_i^2}{t_{ij}^c [t_i^{qos} r_{ij} - a_{ij}(D_i + t_{ij}^w r_{ij})]}$ for simplification.

2) Obtaining $\boldsymbol{\mu}^*$ to Maximize $g(\boldsymbol{\mu})$: Solving dual problem (33) means obtaining $\boldsymbol{\mu}^*$ in their defined domain to maximize $g(\boldsymbol{\mu})$. In accordance with eq. (35a)-(35c), we first put eq. (35b) into problem (33), thus we obtain

$$\max_{\boldsymbol{\mu}} \ g(\boldsymbol{\mu}) = \sum_{i=1}^{N} [-(\sum_{t=1}^{M} \frac{a_{ij} {t_{ij}^c}^2}{4\kappa_i F_i})\mu_i^2 + F_i \mu_i] \tag{36a}$$

$$\text{s.t. } b_{ij} \le \mu_i \le \frac{2\kappa_i F_i f_{\max}}{t_{ij}^c} \tag{36b}$$

Note that problem (36) can be decomposed into the following N sub problems.

$$\max_{\boldsymbol{\mu}} \ -(\sum_{t=1}^{M} \frac{a_{ij} {t_{ij}^c}^2}{4\kappa_i F_i})\mu_i^2 + F_i \mu_i \quad \text{s.t. (36b)} \tag{37}$$

According to the monotonicity of objective quadratic function, one can have $\boldsymbol{\mu}^*$ under the constraint (36b). Similarly, we can obtain $\boldsymbol{\mu}^*$ under the constraint (35a) and (35c), thus the optimal solution to $\boldsymbol{\mu}^*$ is

$$\mu_{i,a}^* = \begin{cases} b_{ij} & \sum_{t=1}^{M} \frac{a_{ij}^2 r_{ij} t_{ij}^c}{t_i^{qos} r_{ij} - a_{ij} D_i + t_{ij}^w r_{ij}} < 1 \\ 0 & otherwise \end{cases} \tag{38}$$

For brevity, we define $\beta_i = \sum_{t=1}^{M} \frac{a_{ij} {t_{ij}^c}^2}{4\kappa_i F_i}$, thus we obtain

$$\mu_{i,b}^* = \begin{cases} \frac{2\kappa_i F_i f_{\max}}{t_{ij}^c} & \beta_i < \frac{t_{ij}^c}{4\kappa_i f_{\max}} \\ b_{ij} & \frac{F_i}{2\beta_i} < b_{ij} \\ \frac{F_i}{2\beta_i} & otherwise \end{cases} \tag{39}$$

$$\mu_{i,c}^* = \begin{cases} \frac{2\kappa_i F_i f_{\max}}{t_{ij}^c} & F_i \le \sum_{t=1}^{M} a_{ij} t_{ij}^c f_{\max} \\ +\infty & otherwise \end{cases} \tag{40}$$

Due to (13), $F_i \le \sum_{t=1}^{M} a_{ij} t_{ij}^c f_{\max}$ can always be achieved, thus

$$\mu_{i,c}^* = \frac{2\kappa_i F_i f_{\max}}{t_{ij}^c} \tag{41}$$

Therefore, the optimal solution to $\boldsymbol{F}^*$ can be obtained by

$$f_{ij}^* = \arg\max_{f_{ij}^*,\ \mu_i^*} \{g(f_{ij,a}^*,\ \mu_{i,a}^*),\ g(f_{ij,b}^*,\ \mu_{i,b}^*),\ g(f_{ij,c}^*,\ \mu_{i,c}^*)\} \tag{42}$$

We introduce the optimal computing resources allocation for the IoTDs as Algorithm 2.

Algorithm 2 Optimal computing resources allocation algorithm

1: Use eq. (38), (39) and (41) to obtain $\mu_{i,x}^*$, $\forall i \in \mathcal{N}$, $\forall x \in \{a, b, c\}$;
2: Obtain $f_{ij,x}^*$ in accordance with eq. (35), $\forall i \in \mathcal{N}$, $\forall j \in \mathcal{M}$, $\forall x \in \{a, b, c\}$;
3: Use eq. (42) to obtain f_{ij}^*, $\forall i \in \mathcal{N}$, $\forall j \in \mathcal{M}$;
4: **Return:** The optimal computing resources allocation $\boldsymbol{F}^*$.

D. Hovering Time Minimization

Given any IoTDs association and computing resources allocation $\{\boldsymbol{A}, \boldsymbol{F}\}$, the services sequence $\boldsymbol{S}$ of problem (28) can be optimized by solving the following problem

$$\underset{\boldsymbol{S}}{\text{minimize}} \ P_{uav}^H \sum_{j=1}^{M} c_{Kj}^c \quad \text{s.t. (3)} \tag{43}$$

which can be decomposed and transformed equivalently into the following M independent sub-problems

$$\underset{S_j, \boldsymbol{s}_{kj}, \boldsymbol{c}_{kj}}{\text{minimize}} \ c_{Kj}^c \quad \text{s.t. (3)-(7)} \tag{44}$$

Notice that the three-stage flow-shop problem is a well-known NP-hard problem and it is difficult to find the optimal solution. According to the structure of the proposed TDMA based workflow model, we combine the wireless powering stage with the data uploading stage into one stage called transferring stage which lasts t_{ij}^{tf}. Thus, one can have

$$t_{kj}^{tf} = t_{kj}^w + t_{kj}^u,\ k \in \mathcal{K}_j,\ \forall j \in \mathcal{M} \tag{45}$$

Let s_{kj}^{tf} and c_{kj}^{tf} denote the starting and completion time of the transferring stage, respectively. One can have

$$\begin{cases} s_{kj}^{tf} + t_{kj}^{tf} = c_{kj}^{tf} \\ s_{kj}^c + t_{kj}^c = c_{kj}^c \end{cases},\ k \in \mathcal{K}_j,\ \forall j \in \mathcal{M} \tag{46}$$

$$\begin{cases} s_{kj}^{tf} \ge 0 \\ s_{kj}^c \ge c_{kj}^{tf} \end{cases},\ k \in \mathcal{K}_j,\ \forall j \in \mathcal{M} \tag{47}$$

$$\begin{cases} s_{kj}^{tf} \ge c_{k-1,j}^{tf} \\ s_{kj}^c \ge c_{k-1,j}^c \end{cases},\ k \in \mathcal{K}_j,\ \forall j \in \mathcal{M} \tag{48}$$

Therefore, problem (44) can be simplified into a two-stage flow-shop problem as

$$\underset{S_j, \boldsymbol{s}_{kj}, \boldsymbol{c}_{kj}}{\text{minimize}} \ c_{Kj}^c \quad \text{s.t. (45)-(48)} \tag{49}$$

Let $\boldsymbol{T_1}$ denote the set of $\{t_{kj}^{tf}, \forall k \in \mathcal{K}_j\}$ and $\boldsymbol{T_2}$ denote the set of $\{t_{kj}^c, \forall k \in \mathcal{K}_j\}$. The sequence $\boldsymbol{S}$ of the two-stage flow-shop problem can be solved by exploring the Johnson's algorithm [42] efficiently and optimally. According to Fig. 3 (b), in order to avoid the time gap, one should choose the longer time block between the k-th computing stage and

the (k-1)-th transferring stage to calculate the optimal c_{Kj}^{c*}. Based on this, we develop the novel UAV hovering time minimization algorithm as follows

Algorithm 3 Optimal UAV hovering time minimization algorithm

1: Use eq. (10), (11), (21) and (45) to obtain t_{ij}^{u*}, t_{ij}^{c*}, t_{ij}^{w*} and t_{kj}^{tf*}, let $n=0$, $m=0$;
2: **Repeat:**
3: Find the minimal time $t_{k_{min}}$ in $\boldsymbol{T_1}$ and $\boldsymbol{T_2}$;
4: If $t_{k_{min}} \in \boldsymbol{T_1}$ then $S_{n+1}=k_{min}$, $n=n+1$;
5: else if $t_{k_{min}} \in \boldsymbol{T_2}$ then $S_{K-m}=k_{min}$, $m=m+1$;
6: Remove $t_{k_{min}}^{tf}$ from $\boldsymbol{T_1}$ and $t_{k_{min}}^{c}$ from $\boldsymbol{T_2}$;
7: **Until:** $\boldsymbol{T_1}$ and $\boldsymbol{T_2}=\boldsymbol{\varnothing}$;
8: Update n=1 and $s_1^{tf}=0$;
9: **Repeat:**
10: If $t_{n+1}^{tf} \geq t_n^c$ then $c_{n+1}^c = s_n^{tf}+t_n^{tf}+t_{n+1}^{tf}+t_{n+1}^c$ and $s_{n+1}^{tf}=s_n^{tf}+t_n^{tf}$;
11: If $t_{n+1}^{tf} < t_n^c$ then $c_{n+1}^c = s_n^{tf}+t_n^{tf}+t_n^c+t_{n+1}^c$ and $s_{n+1}^{tf}=s_n^{tf}+t_n^{tf}+t_n^c-t_{n+1}^{tf}$;
12: $n=n+1$;
13: **Until:** $n=K$;
14: $T_j^*=c_{Kj}^c$;
15: **Return:** The optimal services sequence $\boldsymbol{S^*}$ and the optimal UAV hovering durations $\boldsymbol{t}^*$ for $\mathcal{P}1$.

E. Overall Algorithm

For the non-convex problem, if the object function of the original problem is not block multi-convex [43], the result of the conventional iterative method (i.e. block-coordinate descent method) is relevant to the initial iteration point. Therefore, we design an adaptive method to set the initial iteration point by observing the structures of problem (29) and (30).

For problem (29), the object function (29a) is the weighted sum of the variables a_{ij}. Let w_{ij} denote the weighted value

$$w_{ij}=\kappa_i F_i(f_{ij})^2+p_i D_i/[B\log_2\left(1+\frac{p_i h_{ij}}{\sigma^2}\right)] \tag{50}$$

Notice that, according to the structure of problem (29), $a_{ij}=1$ if and only if w_{ij} is minimal. Note that for each i-th IoTD w_{ij} is a function of h_{ij} and f_{ij}. Furthermore, one can see that according to the structure of problem (30), with the increase of h_{ij}, the lower bound of f_{ij} decreases correspondingly. Also, if h_{ij} increases and f_{ij} decreases, the value of w_{ij} will decrease. That means if $a_{ij}^0=1$, $\boldsymbol{A}^0$ will be closer to the optimal point $\boldsymbol{A}^*$ when the value of h_{ij} is greater. Therefore, given any i, we set the initial point of $\boldsymbol{A}^0$ using the following equation

$$a_{ij}^0=\begin{cases}1 & h_{ij}=\max\{h_{ij},\forall i\in\mathcal{N},\forall j\in\mathcal{M}\}\\ 0 & otherwise\end{cases} \tag{51}$$

Based on the previous results, we propose the overall iterative algorithm for the original problem $\mathcal{P}1$ as Algorithm 4.

Algorithm 4 The proposed overall iterative method based algorithm for $\mathcal{P}1$

1: **Initialize:** Use eq. (51) to obtain $\boldsymbol{A}^0$ and set a random $\boldsymbol{S}^0$. Let $r=0$.
2: **Repeat:**
3: For given $\{\boldsymbol{A}^r,\boldsymbol{S}^r\}$, use *Algorithm 2* to obtain the optimal solution denoted as $\boldsymbol{F}^{r+1}$;
4: For given $\{\boldsymbol{S}^r,\boldsymbol{F}^{r+1}\}$, use *CVX tool box* to obtain the optimal solution denoted as $\boldsymbol{A}^{r+1}$;
5: For given $\{\boldsymbol{A}^{r+1},\boldsymbol{F}^{r+1}\}$, use *Algorithm 3* to obtain the optimal solution denoted as $\boldsymbol{S}^{r+1}$ and $\boldsymbol{t}^{r+1}$;
6: Use eq. (9) to obtain the optimal data rate denoted as $\boldsymbol{r}^{r+1}$;
7: Update $r=r+1$.
8: **Until:** The fractional decrease of E is below a threshold ϵ or a maximum number of iterations ($r_{\max}$) is reached;
9: **Return:** The optimal IoTDs association $\boldsymbol{A^*}$, computing resources allocation $\boldsymbol{F^*}$, the uplink data rate $\boldsymbol{r}^*$, UAV hovering durations $\boldsymbol{t^*}$ and the services sequence of the IoTDs $\boldsymbol{S^*}$.

The computation complexity analysis of Algorithm 4 is shown as follows. In each iteration, the IoTDs association and the hovering time minimization are sequentially optimized using the CVX (based on the interior-point method) and the Johnson's algorithm. Thus, given the solution accuracy of $\epsilon>0$, their individual complexity can be represented by $\mathcal{O}((NM)^{3.5}log(1/\epsilon))$ and $\mathcal{O}(nlog(n))$, respectively. Accounting for the BCD iterations with the complexity in the order of $log(1/\epsilon)$, the total computation complexity of Algorithm 4 is thus $\mathcal{O}((NM)^{3.5}log^2(1/\epsilon))$. In other words, Algorithm 4 can converge to an optimum solution with a polynomial time computational complexity.

VI. Simulation Results

In this section, we provide the simulation results to demonstrate the effectiveness of the proposed algorithm. We consider the system with one UAV and multiple IoTDs with different tasks, which are randomly and uniformly distributed within a 2D area of 100 × 100 m^2. Considering the statistic relevance of the simulation, the results in Section VI are obtained by 3000 simulation runs with random locations of the IoTDs and their tasks. The UAV hovers above the IoTDs at 8 given locations with the fixed altitude H = 5 m. We set the bandwidth B = 10 MHz, the channel power gain at the reference distance of 1 m as - 30 dB and the noise power at each IoTD as - 60 dBm. The low cost UAV's maximum computation capacity, which can be allocated to a IoTD, is set as 0.5 G CPU cycles per second. The transmission power of each IoTD is set as 200 mW. The power of the UAV WPT antenna is set as 50 dBm. We set the effective switched capacitance $\kappa_i=10^{-26}$. The UAV hovering power consumption is set as P_{uav}^H = 59.2 W [44].

In Fig.4, Fig.7 and Fig. 8, we set the number of IoTDs as 200 while we consider the large scale scenario with up to 1200 IoTDs in Fig.5 and Fig. 6, respectively. The performance

with different number of devices in Fig.5 and Fig. 6 can be obtained by changing the number of devices in the simulation while other simulation parameters remain the same.

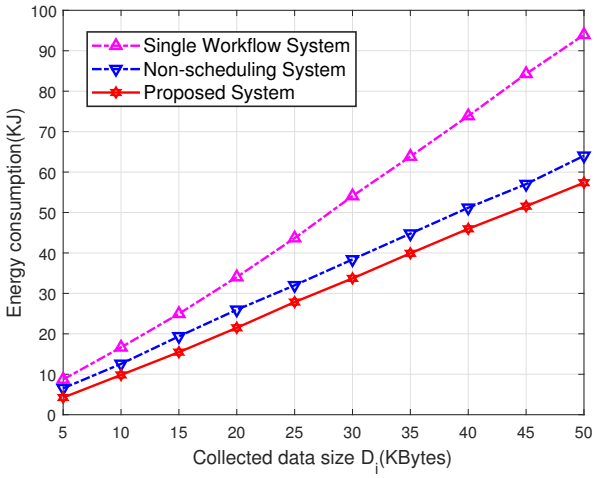

Fig. 4. The UAV energy consumption versus the IoTD sensed data size D_i.

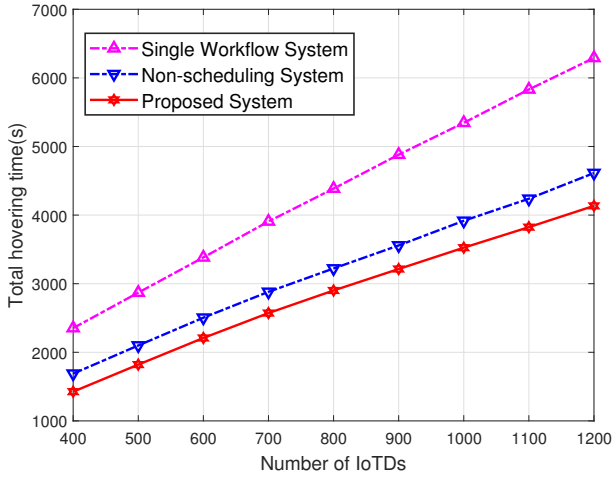

Fig. 5. The UAV hovering time versus the number of IoTDs N.

In Fig.4 and Fig.5, we show the energy-effectiveness and the time-effectiveness of our proposed system, respectively. We compare our proposed UAV system with the conventional single workflow UAV system and the non-scheduling system benchmarks. The non-scheduling system means the system has multi-workflow but without sequence scheduling. One can see that with the increase of the uploaded data from each IoTD, the UAV's energy consumption rises correspondingly.

In Fig. 5, We set the IoTD sensed data size D_i as 50 KBytes. One can see that with the increase of the number of the IoTDs, the UAV hovering time rises as well, as expected. One can also see that in both figures, our proposed system outperforms the other two benchmarks.

Moreover, according to Fig. 6, with the increase of the number of the IoTDs, the UAV hovering time saved rises as well, as expected. Notice that the hovering time saved by the multi-workflow structure with and without scheduling account

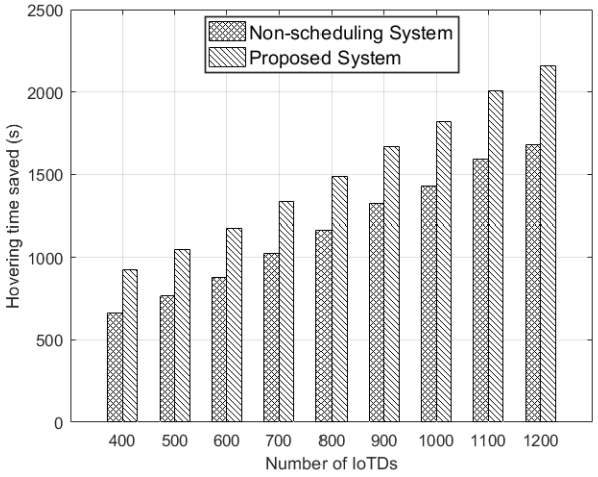

Fig. 6. Hovering time saved versus the number of IoTDs N.

for about 25% and 35% in the single workflow UAV-assisted system, respectively.

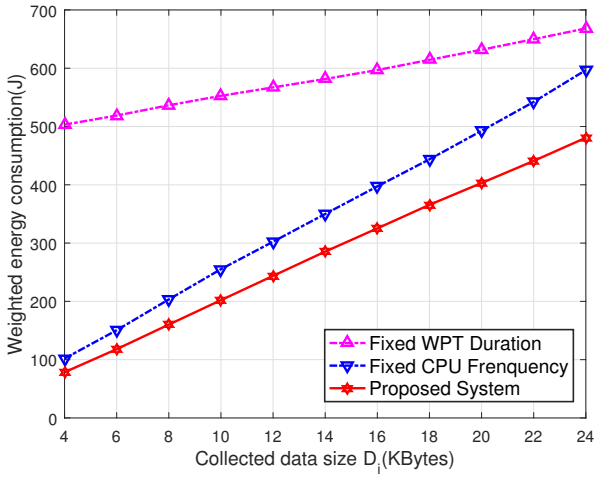

Fig. 7. The weighted UAV energy consumption versus the IoTD sensed data size D_i.

In Fig. 7, we plot the weighted UAV energy consumption versus the IoTD sensed data size D_i. One can see that with the increase of the uploaded data from each IoTD, the weighted UAV's energy consumption rises correspondingly. The Fixed WPT Duration benchmark sets the WPT duration fixed as 1/5 t_i^{qos} and the Fixed CPU Frequency benchmark sets the frequency fixed as f_{max}. In Fig.7, we set the optimization weight φ as 1 and ϕ as 0.01 in $\mathcal{P}1$. Note that the multi-workflow system structure is applied in Fig. 7.

According to Fig. 8, with the increase of the IoTD sensed data size D_i, the UAV total hovering time rises as well, as expected. Furthermore, one can see that with the decrease of the WPT power conversion efficiency v_i, the UAV total hovering time rises, as expected.

In Fig. 9, we set the number of IoTDs as 50. One can see from Fig. 9 that with the increase of the IoTD sensed data size D_i, the UAV total hovering time rises as well, as

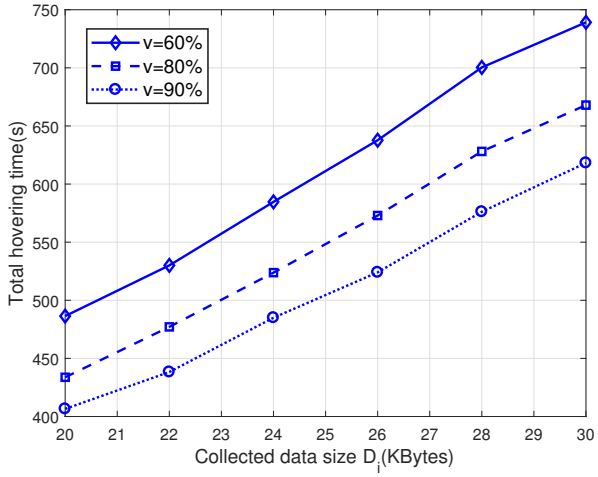

Fig. 8. The UAV hovering time versus the IoTD sensed data size D_i.

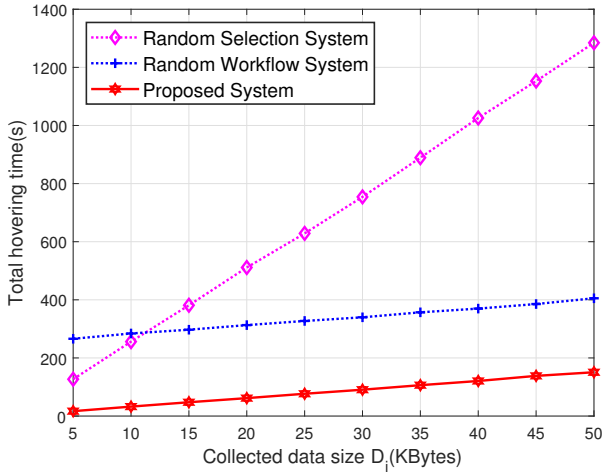

Fig. 9. The UAV hovering time versus the IoTD sensed data size D_i.

expected. The Random Selection System means the IoTDs select the UAV hovering location randomly. In the Random Workflow System, the random workflows may contain some gap time, thus each workflow is poorly ordered, which has been depicted as Fig. 3 (a) in Section III. One can see that the UAV total hovering time is significantly reduced by the proposed Algorithms.

In Fig. 10, we set the number of the IoTDs as 5 and compare our proposed solution with the exhaustive search. The exhaustive search can be considered as the optimal solution. However, it just searches all the feasible solutions, which has the lowest efficiency. One can see that the performance of our algorithm is close to the exhaustive algorithm but we have much less complexity.

VII. Conclusion

In this paper, we investigate how the UAV should optimally exploits its mobility via hovering design. We formulate the UAV minimization problem as a mixed-integer non-convex problem, which is difficult to solve. We transform it into

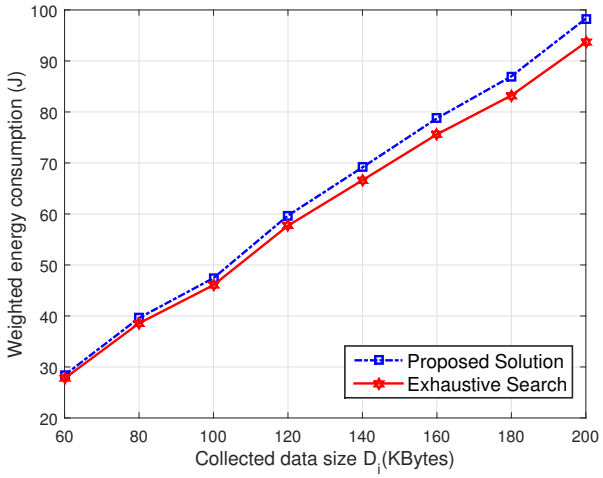

Fig. 10. The gap between the optimal solution and our proposed suboptimal solution.

a tractable one which can be solved by using the convex optimization and the flow-shop scheduling techniques. Furthermore, we develop an alternative algorithm which initial point can be set closer to the optimal solution adaptively. Simulation results show that the energy efficiency is enhanced greatly compared with the conventional UAV-assisted system.

Appendix A
Proof of Theorem 1

Proof. Notice that the object function of problem (19) consists of three independent parts, including the computing energy, the wireless powering energy and the hovering energy. With the decrease of the UAV hovering time T_j, the hovering energy consumption decreases as well. Therefore, the optimal T_j is obtained when the equality holds for the constraint (19g). The proof for Theorem 1 is complete. □

Appendix B
Proof of Theorem 2

Proof. The object function of problem (27) consists of three independent parts, including the computing energy, the wireless powering energy and the hovering energy. Therefore, problem (27) can be decomposed into $N \times M$ independent sub-problems of the wireless powering durations $\boldsymbol{\tau}$. The object function (27a) is minimal when the equality of the wireless powering energy constraint holds for (15), thus we prove Theorem 2. □

Appendix C
Proof of Theorem 3

Proof. Note that problem (23) can be decomposed into the following $N \times M$ subproblems.

$$\underset{\boldsymbol{F}}{\text{minimize}}\ \varphi\kappa_i F_i a_{ij} {f_{ij}}^2 + \frac{\phi P_{uav}^H a_{ij} F_i}{f_{ij}} \tag{52a}$$

$$\text{s.t. } f_{ij}^l \le f_{ij} \le f_{max} \tag{52b}$$

Let $\mathscr{F}(f_{ij}) = \varphi\kappa_i F_i a_{ij} {f_{ij}}^2 + \frac{\phi P_{uav}^H a_{ij} F_i}{f_{ij}}$

$$\frac{\partial \mathscr{F}}{\partial f_{ij}} = 2\varphi\kappa_i F_i a_{ij} f_{ij} - \frac{\phi P_{uav}^H a_{ij} F_i}{{f_{ij}}^2} \tag{53}$$

$$\frac{\partial^2 \mathscr{F}}{\partial {f_{ij}}^2} = 2\varphi\kappa_i F_i a_{ij} + \frac{2\phi P_{uav}^H a_{ij} F_i}{{f_{ij}}^3} \tag{54}$$

According to equation (54), the second order derivative of $\mathscr{F}$ is no less than zero, therefore, function $\mathscr{F}$ is convex. Furthermore, the object function of problem (23) is the sum of convex functions, therefore, problem (23) is a convex problem. Let $\frac{\partial \mathscr{F}}{\partial f_{ij}} = 0$, one can have

$$f_{ij}^* = \sqrt[3]{\frac{\phi P_{uav}^H}{2\varphi\kappa_i}} \quad f_{ij}^l \leq \sqrt[3]{\frac{\phi P_{uav}^H}{2\varphi\kappa_i}} \leq f_{max} \tag{55}$$

Moreover, according to equation (53) when $\sqrt[3]{\frac{\phi P_{uav}^H}{2\varphi\kappa_i}} < f_{ij}^l$, the first order derivative of $\mathscr{F}$ is greater than zero, which means $\mathscr{F}$ is monotone increasing. Also, when $\sqrt[3]{\frac{\phi P_{uav}^H}{2\varphi\kappa_i}} > f_{max}$, the first order derivative of $\mathscr{F}$ is less than zero, which means $\mathscr{F}$ is monotone decreasing. Therefore, equation (24) is proved. The proof for Theorem 3 is complete. □

REFERENCES

[1] Y. Mao, C. You, J. Zhang, K. Huang, and K. B. Letaief, "A survey on mobile edge computing: The communication perspective," *IEEE Communications Surveys & Tutorials*, vol. 19, no. 4, pp. 2322–2358, Nov. 2017.

[2] H. Guo and J. Liu, "Collaborative computation offloading for multiaccess edge computing over fiber–wireless networks," *IEEE Transactions on Vehicular Technology*, vol. 67, no. 5, pp. 4514–4526, May 2018.

[3] K. Wang, K. Yang, H. Chen, and L. Zhang, "Computation diversity in emerging networking paradigms," *IEEE Wireless Communications*, vol. 24, no. 1, pp. 88–94, Feb. 2017.

[4] S. Bi, C. K. Ho, and R. Zhang, "Wireless powered communication: Opportunities and challenges," *IEEE Communications Magazine*, vol. 53, no. 4, pp. 117–125, Apr. 2015.

[5] S. Hayat, E. Yanmaz, and R. Muzaffar, "Survey on unmanned aerial vehicle networks for civil applications: A communications viewpoint," *IEEE Communications Surveys & Tutorials*, vol. 18, no. 4, pp. 2624–2661, Nov. 2016.

[6] X. Yang, P. Chen, S. Gao, and Q. Niu, "CSI-based low-duty-cycle wireless multimedia sensor network for security monitoring," *Electronics Letters*, vol. 54, no. 5, pp. 323–324, Mar. 2018.

[7] X. Lin, V. Yajnanarayana, S. D. Muruganathan, S. Gao, H. Asplund, H. L. Maattanen, M. Bergstrom, S. Euler, and Y. P. E. Wang, "The sky is not the limit: LTE for unmanned aerial vehicles," *IEEE Communications Magazine*, vol. 56, no. 4, pp. 204–210, Apr. 2018.

[8] S. Jeong, O. Simeone, and J. Kang, "Mobile edge computing via a UAV-mounted cloudlet: Optimization of bit allocation and path planning," *IEEE Transactions on Vehicular Technology*, vol. 67, no. 3, pp. 2049–2063, Mar. 2018.

[9] K. Yang, S. Ou, and H. Chen, "On effective offloading services for resource-constrained mobile devices running heavier mobile internet applications," *IEEE Communications Magazine*, vol. 46, no. 1, pp. 56–63, Jan. 2008.

[10] K. Wang, K. Yang, and C. S. Magurawalage, "Joint energy minimization and resource allocation in C-RAN with mobile cloud," *IEEE Transactions on Cloud Computing*, vol. 6, no. 3, pp. 760–770, Jul. 2018.

[11] C. Zhan, Y. Zeng, and R. Zhang, "Energy-efficient data collection in UAV enabled wireless sensor network," *IEEE Wireless Communications Letters*, vol. 7, no. 3, pp. 328–331, Jun. 2018.

[12] J. Xu, Y. Zeng, and R. Zhang, "UAV-enabled wireless power transfer: Trajectory design and energy optimization," *IEEE Transactions on Wireless Communications*, vol. 17, no. 8, pp. 5092–5106, Aug. 2018.

[13] F. Zhou, Y. Wu, R. Q. Hu, and Y. Qian, "Computation rate maximization in UAV-enabled wireless-powered mobile-edge computing systems," *IEEE Journal on Selected Areas in Communications*, vol. 36, no. 9, pp. 1927–1941, Sep. 2018.

[14] J. Guo, Z. Song, Y. Cui, Z. Liu, and Y. Ji, "Energy-efficient resource allocation for multi-user mobile edge computing," in *2017 IEEE Global Communications Conference (GLOBECOM)*, Dec. 2017, pp. 1–7.

[15] C. Luo, S. I. McClean, G. Parr, L. Teacy, and R. De Nardi, "UAV position estimation and collision avoidance using the extended Kalman filter," *IEEE Transactions on Vehicular Technology*, vol. 62, no. 6, pp. 2749–2762, Jul. 2013.

[16] F. Tang, Z. M. Fadlullah, N. Kato, F. Ono, and R. Miura, "AC-POCA: Anticoordination game based partially overlapping channels assignment in combined UAV and D2D-based networks," *IEEE Transactions on Vehicular Technology*, vol. 67, no. 2, pp. 1672–1683, Feb. 2018.

[17] G. Zhang, K. Yang, P. Liu, and J. Wei, "Power allocation for full-duplex relaying-based D2D communication underlaying cellular networks," *IEEE Transactions on Vehicular Technology*, vol. 64, no. 10, pp. 4911–4916, Oct. 2015.

[18] L. Xiao, X. Lu, D. Xu, Y. Tang, L. Wang, and W. Zhuang, "UAV relay in VANETs against smart jamming with reinforcement learning," *IEEE Transactions on Vehicular Technology*, vol. 67, no. 5, pp. 4087–4097, May 2018.

[19] T. Yu, X. Wang, J. Jin, and K. McIsaac, "Cloud-orchestrated physical topology discovery of large-scale IoT systems using UAVs," *IEEE Transactions on Industrial Informatics*, vol. 14, no. 5, pp. 2261–2270, May 2018.

[20] M. A. Abd-Elmagid and H. S. Dhillon, "Average peak age-of-information minimization in UAV-assisted IoT networks," *IEEE Transactions on Vehicular Technology*, vol. 68, no. 2, pp. 2003–2008, Feb. 2019.

[21] D. Takaishi, Y. Kawamoto, H. Nishiyama, N. Kato, F. Ono, and R. Miura, "Virtual cell based resource allocation for efficient frequency utilization in unmanned aircraft systems," *IEEE Transactions on Vehicular Technology*, vol. 67, no. 4, pp. 3495–3504, Apr. 2018.

[22] S. Yan, M. Peng, and X. Cao, "A game theory approach for joint access selection and resource allocation in UAV assisted IoT communication networks," *IEEE Internet of Things Journal*, vol. 6, no. 2, pp. 1663–1674, Apr. 2019.

[23] M. Mozaffari, W. Saad, M. Bennis, and M. Debbah, "Mobile unmanned aerial vehicles (UAVs) for energy-efficient internet of things communications," *IEEE Transactions on Wireless Communications*, vol. 16, no. 11, pp. 7574–7589, Nov. 2017.

[24] K. Wang, P. Huang, K. Yang, C. Pan, and J. Wang, "Unified offloading decision making and resource allocation in ME-RAN," *IEEE Transactions on Vehicular Technology*, pp. 1–14, DOI: 10.1109/TVT.2019.2926513 (Early Access).

[25] K. Yang, S. Ou, K. Guild, and H. Chen, "Convergence of ethernet PON and IEEE 802.16 broadband access networks and its QoS-aware dynamic bandwidth allocation scheme," *IEEE Journal on Selected Areas in Communications*, vol. 27, no. 2, pp. 101–116, Feb. 2009.

[26] T. G. Rodrigues, K. Suto, H. Nishiyama, and N. Kato, "Hybrid method for minimizing service delay in edge cloud computing through VM migration and transmission power control," *IEEE Transactions on Computers*, vol. 66, no. 5, pp. 810–819, May 2017.

[27] T. G. Rodrigues, K. Suto, H. Nishiyama, N. Kato, and K. Temma, "Cloudlets activation scheme for scalable mobile edge computing with transmission power control and virtual machine migration," *IEEE Transactions on Computers*, vol. 67, no. 9, pp. 1287–1300, Sep. 2018.

[28] Y. Du, K. Wang, K. Yang, and G. Zhang, "Energy-efficient resource allocation in UAV based MEC system for IoT devices," in *2018 IEEE Global Communications Conference (GLOBECOM)*, Dec. 2018, pp. 1–6.

[29] F. Tang, Z. M. Fadlullah, B. Mao, N. Kato, F. Ono, and R. Miura, "On a novel adaptive UAV-mounted cloudlet-aided recommendation system for LBSNs," *IEEE Transactions on Emerging Topics in Computing*, pp. 1–13, DOI: 10.1109/TETC.2018.2792051 (Early Access).

[30] Y. Zhao, J. Hu, Z. Ding, and K. Yang, "Joint interleaver and modulation design for multi-user swipt-noma," *IEEE Transactions on Communications*, pp. 1–1, 2019.

[31] J. Hu, J. Luo, Y. Zheng, and K. Li, "Graphene-grid deployment in energy harvesting cooperative wireless sensor networks for green IoT," *IEEE Transactions on Industrial Informatics*, vol. 15, no. 3, pp. 1820–1829, Mar. 2019.

[32] S. Cho, K. Lee, B. Kang, K. Koo, and I. Joe, "Weighted harvest-then-transmit: UAV-enabled wireless powered communication networks," *IEEE Access*, vol. 6, pp. 72 212–72 224, Nov. 2018.

[33] L. Xie, J. Xu, and R. Zhang, "Throughput maximization for UAV-enabled wireless powered communication networks," *IEEE Internet of Things Journal*, vol. 6, no. 2, pp. 1690–1703, Apr. 2019.

[34] K. Lv, J. Hu, Q. Yu, and K. Yang, "Throughput maximization and fairness assurance in data and energy integrated communication networks," *IEEE Internet of Things Journal*, vol. 5, no. 2, pp. 636–644, Apr. 2018.

[35] F. Zhou, Y. Wu, H. Sun, and Z. Chu, "UAV-enabled mobile edge computing: Offloading optimization and trajectory design," in *2018 IEEE International Conference on Communications (ICC)*, May 2018, pp. 1–6.

[36] L. Yang, J. Cao, S. Tang, T. Li, and A. T. S. Chan, "A framework for partitioning and execution of data stream applications in mobile cloud computing," in *2012 IEEE Fifth International Conference on Cloud Computing*, Jun. 2012, pp. 794–802.

[37] Y. Sun, D. Xu, D. W. K. Ng, L. Dai, and R. Schober, "Optimal 3D-trajectory design and resource allocation for solar-powered UAV communication systems," *IEEE Transactions on Communications*, vol. 67, no. 6, pp. 4281–4298, Jun. 2019.

[38] K. Wang and K. Yang, "Power-minimization computing resource allocation in mobile cloud-radio access network," in *2016 IEEE International Conference on Computer and Information Technology (CIT)*, Dec. 2016, pp. 667–672.

[39] Y. Zeng, X. Xu, and R. Zhang, "Trajectory design for completion time minimization in UAV-enabled multicasting," *IEEE Transactions on Wireless Communications*, vol. 17, no. 4, pp. 2233–2246, Apr. 2018.

[40] M. Grant and S. Boyd., "CVX: Matlab software for disciplined convex programming, version 3.0," *(Jun. 2015)*, Available: http://cvxr.com/cvx.

[41] S. Boyd and L. Vandenberghe, *Convex Optimization*. Cambridge Univ. Press, U.K., 2004.

[42] S. M. Johnson, "Optimal two-and three-stage production schedules with setup times included," *Naval research logistics quarterly*, vol. 1, no. 1, pp. 61–68, Mar. 1954.

[43] Y. Xu and W. Yin, "A block coordinate descent method for regularized multiconvex optimization with applications to nonnegative tensor factorization and completion," *SIAM Journal on imaging sciences*, vol. 6, no. 3, pp. 1758–1789, Sep. 2013.

[44] J. Gundlach, *Designing Unmanned Aircraft Systems: A Comprehensive Approach*. American Institute of Aeronautics and Astronautics. Press, U.S.A., 2012.

Yao Du received the B.S. in communication engineering from China University of Mining and Technology in 2017. He is currently pursuing the M.S. degree with the School of Information and Communication Engineering in University of Electronic Science and Technology of China. His research interests include mobile edge computing, unmanned aerial vehicle and convex optimization.

Kun Yang received his PhD from the Department of Electronic & Electrical Engineering of University College London (UCL), UK, and MSc and BSc from the Computer Science Department of Jilin University, China. He is currently a Chair Professor in the School of Computer Science & Electronic Engineering, University of Essex, leading the Network Convergence Laboratory (NCL), UK. He is also an affiliated professor at UESTC, China. Before joining in University of Essex at 2003, he worked at UCL on several European Union (EU) research projects for several years. His main research interests include wireless networks and communications, data and energy integrated networks, computation and communication cooperation. He manages research projects funded by various sources such as UK EPSRC, EU FP7/H2020 and industries. He has published 150+ journal papers. He serves on the editorial boards of both IEEE and non-IEEE journals. He is a Senior Member of IEEE (since 2008) and a Fellow of IET (since 2009).

Kezhi Wang received his B.E. and M.E. degrees in School of Automation from Chongqing University, China, in 2008 and 2011, respectively. He received his Ph.D. degree in Engineering from the University of Warwick, U.K. in 2015. He was a senior research officer in University of Essex, U.K. Currently he is a Lecturer with Department of Computer and Information Sciences at Northumbria University, U.K. His research interests include wireless communication, mobile edge computing and machine learning.

Guopeng Zhang received the bachelor's degree from the School of Computer Science, Jiangsu Normal University, China, in 2001, the master's degree from the School of Computer Science, South China Normal University, China, in 2005, and the Ph.D. degree from the School of Communication Engineering, Xidian University, China, in 2009. He was with ZTE Corporation Nanjing Branch for one year. In 2009, he joined the China University of Mining and Technology, China, where he is currently a Professor with the School of Computer Science and Technology. He manages research projects funded by various sources, such as the National Natural Science Foundation of China. He has published more than 60 journal and conference papers. His main research interests include wireless sensor networks, wireless personal area networks, and their applications in the Internet of Things.

Yizhe Zhao (S'16) received the B.S. in communication engineering from Xidian University in 2014, and the M.S. in information and communication engineering from University of Electronic Science and Technology of China (UESTC) in 2017. He is currently pursuing the Ph.D. degree with the School of Information and Communication Engineering in UESTC. He has been a Visiting Researcher with the Department of Electrical and Computer Engineering, University of California, Davis, USA. His research focuses on simultaneous wireless information and power transfer, data and energy integrated communication networks as well as machine learning.

Dongwei Chen is an associate professor in School of Electronic Information Engineering, University of Electronic Science and Technology of China, Zhongshan Institute. He is the director of Brain-Like Computing and Intelligent Robotics (BCIR) Lab at UESTC-ZSC. He is a senior member of CCF. He is also the member of IEEE-CS and ACM. He is Talent of Thousands of Talents Training Project in GuangDong High Education. He is Head of Computing Group of Wireless Energy Transfer Flexible IoT Innovation Research Team in Zhongshan. He is the Smart Home Incubator Business Mentor of China Smart Home Industry Alliance (CSHIA) . He has published more than 20 papers, including SCI/EI index. He hosts more than 10 research projects of the provincial and civic government department and enterprise. He has obtained one invention patent, two utility model patent and three copyrights in computer software. His research focuses on Brain-Like Computing, Emotion Communications and Intelligent Robotics, Healthcare Big Data, and Body Area Networks, etc.